

Two general solutions of torsional compliance for variable rectangular cross-section hinges in compliant mechanisms

Guimin Chen^{a,b,*}, Larry L. Howell^b

^a School of Mechatronics, Xidian University, Xi'an, Shaanxi 710071, China

^b Mechanical Engineering Department, Brigham Young University, Provo, UT 84602, USA

ARTICLE INFO

Article history:

Received 10 March 2008

Received in revised form 17 July 2008

Accepted 28 August 2008

Available online 6 September 2008

Keywords:

Torsional compliance

Variable rectangular cross-section beam

Compliant mechanism

ABSTRACT

Several approaches exist for calculating the torsional compliance of rectangular cross-section beams, but most depend on the relative magnitude of the cross-section thickness and width, which might be changing during the design phase (especially for design optimization) or is variant for variable cross-section beams such as circular flexure hinges and tapered bars. After summarizing current equations and analyzing their computational accuracy, two new equations are proposed, which are thickness-to-width ratio independent, and suitable for variable cross-section beams and optimization design of torsional elements in compliant mechanisms. The closed-form equations for the torsional compliance of elliptical and circular flexure hinges are derived by using the new equations.

© 2008 Elsevier Inc. All rights reserved.

1. Introduction

Elastic deformation due to torsion is a valuable and often-used approach for producing motion in many devices, including compliant mechanisms and compliant microelectromechanical systems (MEMS). Jacobsen et al. [1] used torsion to achieve out-of-plane motion in lamina emergent mechanisms. Goldfarb et al. [2] designed a “split-tube” flexure which is based on the torsion of the open-section hollow shaft. Degani et al. [3] and Bao et al. [4] researched torsion micromirrors, which have been used in various MEMS such as optical displays and optical switches. Torsion elements have been employed in many compliant mechanisms [5]. The design of torsion elements or modules is of practical importance in many current and future compliant mechanism applications.

The flexure hinges in some compliant mechanisms are subject to unexpected moments created by torsion. For example, although a single-axis circular flexure hinge is designed to primarily have large compliance about its input axis, the torsional compliance is comparable in magnitude. Therefore, the torsional compliance of single-axis flexure hinges should be treated carefully, especially in spatial compliant mechanisms.

There are several equations available to calculate the torsion of rectangular cross-section beams. Before using these equations, one

of the two dimensions of the cross-section (for example the thickness) must be defined as the wider of the two dimensions. This is because the dimensions in the equations do not refer to geometry in a specific direction (e.g. the width in the x direction), but rather refer to the relative magnitude of the dimensions (i.e., which is the smallest dimension). However, many applications use variable cross-section beams such as circular flexure hinges and tapered bars. Sometimes the cross-section varies, and the relative magnitude of the two dimensions changes. Fig. 1 shows a tapered bar, whose width is w and thickness is t . $t > w$ holds for the part left of point “S” (the “switch point”), while $t < w$ elsewhere. In this case, the equations are not adequate for the full length of the beam. At the switch point where the largest dimension switches, the variables in the equation will also have to switch.

In addition, the thickness-to-width ratio of the beam(s) subject to torsion in a mechanism may change greatly during the design iteration process. This is especially true for an optimization design process. When optimizing, currently available equations require switching the variables at the switch point. Thus, an equation that is valid regardless of the width-to-thickness ratio would be advantageous in automating the design of the flexures using optimization and in better understanding their behavior.

The modeling effort on torsional compliance for variable cross-section flexure hinges is possible because of previous work on torsion hinges. Koseki et al. [6] studied the torsional compliance for constant rectangular cross-section flexures. Based on the simplified Young's torsion equation [7], Lobontiu et al. [8–10] formulated the closed-form torsional compliance equations for several variable

* Corresponding author at: School of Mechatronics, Xidian University, No. 2, South Taibai Road, Xi'an, Shaanxi 710071, China.

E-mail address: guimin.chen@gmail.com (G. Chen).

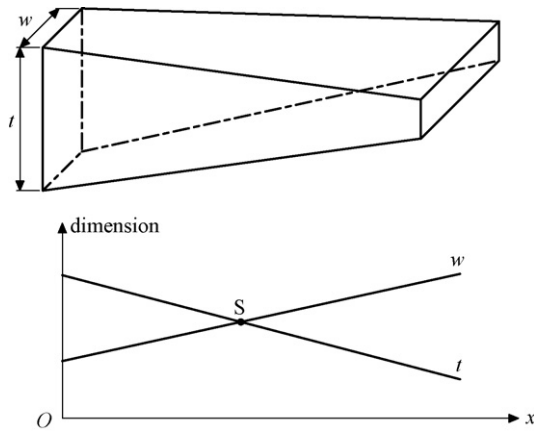


Fig. 1. A tapered rectangular cross-section bar.

cross-section hinges by assuming that the thickness-to-width ratio is equal to or larger than 1 (or equal to or less than 1) for the whole notch region.

The present work compares different torsional equations for rectangular cross-section bars, and proposes two precise and effective equations that is independent of the thickness-to-width ratio. Based on these equations, torsional compliance equations for elliptical and circular flexure hinges are derived.

2. Torsion compliance of flexure hinges

Flexure hinges [11] in various forms find wide use in a variety of compliant mechanisms such as micro-grabbers, micro-positioning stages, high-accuracy alignment devices, displacement amplifiers and parallel micromechanisms because they are small in size, high in sensitivity, and without mechanical friction and backlash.

The cutout profile selection and parameter design of flexure hinges are two important aspects in the process of compliant mechanism design. Although circular flexures are often used, there are many applications where other kinds of hinges are preferable. For example, elliptical flexures were used in displacement amplifiers of large amplification factors and long-travel micro-positioning stages. Compared with circular flexures, elliptical flexures distribute the deformation more evenly over the length of the hinge, thus lowering stress concentrations and achieving larger compliance for a given hinge length [12]. Larger compliance means less force is needed to actuate the mechanism, while lower stress concentrations mean reducing the probability of fatigue failure and thus prolonging the life of the mechanism.

Fig. 2 illustrates an elliptical flexure hinge, where “ t_0 ” denotes the minimum thickness of the hinge, “ w ” denotes the hinge width, a and b are the two semi-axes of the notch ellipse, and $t(x)$ is the variable thickness of the notch region which varies along the notch region. Two special cases of elliptical hinges are shown in Fig. 2, i.e., a circular hinge (where $a = b$) and a leaf-type hinge (where $b = 0$). The torsional compliance equation for elliptical flexure hinges derived in this paper also applies to circular hinges.

Assume that the flexure hinge is fixed at one end, while the torsion load is applied at the opposite, free end. Denote the torsion angle due to pure torsion M_x by α_x , which can be expressed as

$$\alpha_x = \int_0^l \frac{M_x}{GI(x)} dx, \quad (1)$$

where l is the length of the hinge, G is the modulus of rigidity, and $I(x)$ is the torsional moment of inertia for the infinitesimal strip at position x , which depends on the form and dimensions of the

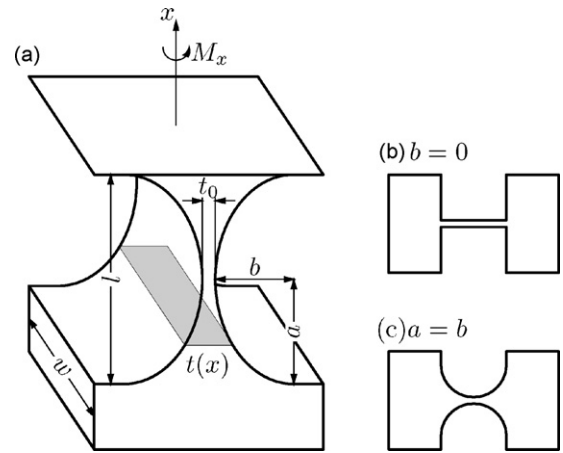


Fig. 2. Elliptical flexure hinges.

cross-section at x . Therefore, the torsional compliance, C , is given by

$$C = \frac{\alpha_x}{M_x} = \int_0^l \frac{1}{GI(x)} dx. \quad (2)$$

For variable rectangular cross-section flexure hinges, each strip of the hinge can be treated as a constant rectangular cross-section beam. There are several methods to calculate $I(x)$, where the calculation accuracy depends on the thickness-to-width ratio ($w/t(x)$) of the hinge. It should be noted that the following three cases are to be considered when calculating $I(x)$ for variable cross-section flexure hinges:

- Case 1: $w \leq t_0$. This is the case dealt with in [10], which often applies for MEMS flexures because of the fabrication methods used.
- Case 2: $w \geq (t_0 + 2b)$. This is the case discussed in [9].
- Case 3: $w \leq (t_0 + 2b)$ while $w \geq t_0$. This is the case where switching w and $t(x)$ is required during the integration (piecewise integration).

3. Different methods for calculation of the torsional moment of inertia I

In this section, the constant-cross-section (i.e., leaf-type) flexure hinge is assumed to simplify the analysis of different equations for calculation of I , that is to say, $b = 0$ or $t(x) = t_0$ for the whole notch region (same as [10]). Thus Eq. (2) can be simplified as

$$C = \frac{l}{GI}. \quad (3)$$

Without loss of generality, we can assume that the thickness-to-width ratio $t_0/w \geq 1$ for the constant cross-section.

3.1. The series solution

The look-up-table method is often used for the torsion calculations for rectangular section beams. The angle of twist, α_x , is given by

$$\alpha_x = \frac{M_x l}{kt_0 w^3 G}, \quad (4)$$

where k is a geometrical constant, whose value depends on the ratio of t_0/w . Table 1 summarizes many representative values of k when $t_0 \geq w$, and is the result of the works of many different authors

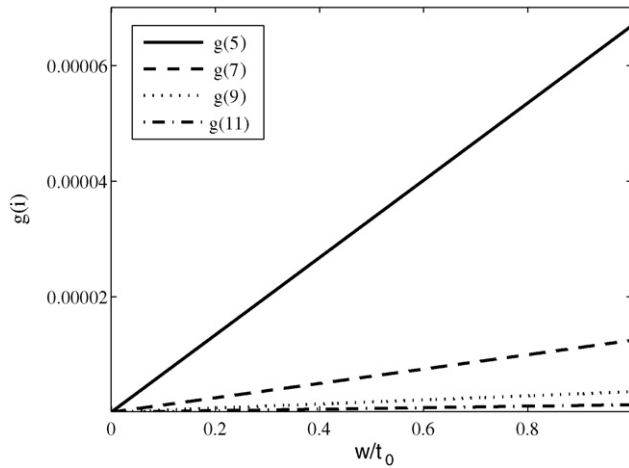


Fig. 3. $g(5)$, $g(7)$, $g(9)$ and $g(11)$ in Eq. (6).

[6,13–19]. Therefore, the corresponding torsional moment of inertia (using the subscript “S” for series solution) can be expressed as

$$I_S = kt_0 w^3. \quad (5)$$

These discrete values are often inadequate for engineering design and a more continuous relationship is needed to calculate the torsional compliance for variable rectangular cross-section beams. In fact, torsion of rectangular sections can be calculated analytically and the result expressed in terms of an infinite series as [20,21]:

$$k = \frac{1}{3} - \frac{64}{\pi^5} \frac{w}{t_0} \sum_{i=1,3,5,\dots}^{\infty} \frac{\tanh(it_0\pi/2w)}{i^5} = \frac{1}{3} - \frac{64}{\pi^5} \frac{w}{t_0} \sum_{i=1,3,5,\dots}^{\infty} g(i) \quad (6)$$

where “tanh” is the hyperbolic tangent function. The series converges rapidly, which can be seen from $g(5)$, $g(7)$, $g(9)$ and $g(11)$ of the series shown in Fig. 3. The results of Eq. (6) agree with the data in Table 1 when the series is added from $i = 1$ to $i = 5$. In the following, we sum the first 500 terms of the series solution (i.e., $i = 1, 3, 5, \dots, 999$) as the exact-form equation for comparisons of various methods.

3.2. The torsion equation: Young and Budynas

Young and Budynas [7] give an approximate equation for the torsional moment of inertia for rectangular cross-sections, which

Table 1
Table of k values for rectangular sections in torsion

t_0/w	k
1.0	0.141
1.2	0.166
1.25	0.172
1.5	0.196
1.75	0.214
2.0	0.229
2.5	0.249
3.0	0.263
4.0	0.281
5.0	0.291
6.0	0.299
8.0	0.307
10.0	0.313
50.0	0.329
∞	0.333

can be expressed as

$$I_Y = t_0 w^3 \left[\frac{1}{3} - 0.21 \frac{w}{t_0} \left(1 - \frac{w^4}{12t_0^4} \right) \right], \quad (7)$$

where the subscript “Y” indicates it was obtained from Young and Budynas’ book [7]. The torsional compliance associated with I_Y is C_Y and is found using Eq. (3). The high-power term in I_Y makes C_Y difficult to integrate in the case of variable cross-section beams. However, numeric integration could be used if high precision is required.

Note that Eq. (7) was incorrectly written in [10] as

$$I_{YL} = t_0 w^3 \left[\frac{1}{3} - 0.21 \frac{w}{t_0} + 0.001 \frac{w^4}{t_0^4} \right]. \quad (8)$$

This transcription error did not result in any problem for the derivation of the simplified equation discussed next, other than the assessment of its accuracy. The corresponding torsional compliance, C_{YL} is found from I_{YL} and Eq. (3).

3.3. The torsion equation: Lobontiu et al.

The width of a flexure hinge is smaller than the minimum thickness in many MEMS applications. In order to deduce the design equations of torsional stiffness of such flexure hinges, Lobontiu et al. [10] simplified Eq. (8) by neglecting the high-power term and reducing the equation to

$$I_L = t_0 w^3 \left[\frac{1}{3} - 0.21 \frac{w}{t_0} \right], \quad (9)$$

where the subscript “L” indicates it was obtained from Lobontiu’s work. The errors caused by neglecting the high-power term are no more than 0.8% when compared to Eq. (8), but unfortunately Eq. (8) is not the correct form of the equation, and the deviation is greater when compared to Eq. (7).

It should be noted that Eqs. (5) to (9) are subject to the assumption of $t_0/w \geq 1$. That is to say, once $t_0/w < 1$, all the w ’s in these equations should be switched to t_0 ’s and all the t_0 ’s should be switched to w ’s.

3.4. The torsion equation: Hearn

Hearn [13] proposed the following approximate form:

$$\frac{\alpha_x}{M_x} = \frac{42LJ}{GA^4} = \frac{L}{G} \frac{42J}{t_0^4 w^4}, \quad (10)$$

where A is the cross-sectional area of the section ($A = wt_0$) and $J = wt_0(w^2 + t_0^2)/12$. From Eq. (10), we can obtain the corresponding approximate equation for the torsional moment of inertia, which can be expressed as

$$I_H = \frac{t_0^4 w^4}{42J} = \frac{2t_0^3 w^3}{7t_0^2 + 7w^2} = \frac{t_0 w^3}{3.5 + 3.5w^2/t_0^2}, \quad (11)$$

where the subscript “H” indicates it was obtained based on the equation presented in Hearn’s book [13]. One of the distinct features of this approximate equation is the symmetric relation between t_0 and w . This means that users do not need to consider whether $t_0/w \geq 1$ or $t_0/w < 1$. In addition, Hearn’s equation is easy to integrate, so it is more suitable for the torsion calculation of variable cross-section beams.

3.5. Error analysis

The torsional compliances calculated by using I_S , I_Y , I_{YL} , I_L and I_H are C_S , C_Y , C_{YL} , C_L and C_H , respectively. The error functions compared

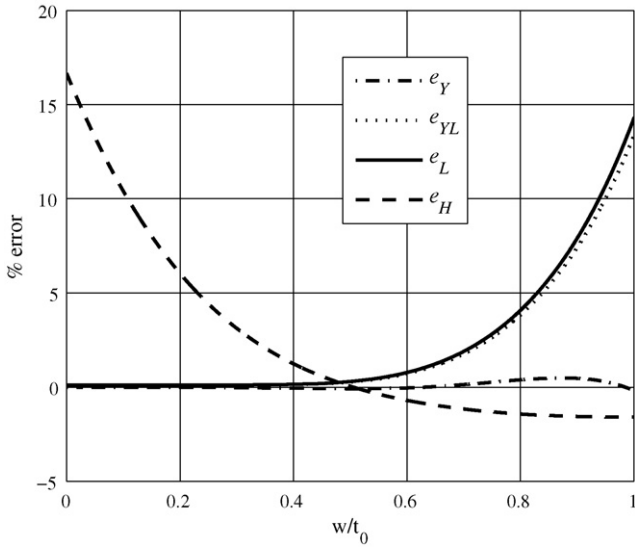


Fig. 4. Errors.

to the torsional compliance calculated by the series equation of Eq. (6)(C_S) can be defined as

$$e_Y = \frac{C_Y - C_S}{C_S} = \frac{I_S}{I_Y} - 1, \quad (12)$$

$$e_{YL} = \frac{C_{YL} - C_S}{C_S} = \frac{I_S}{I_{YL}} - 1, \quad (13)$$

$$e_L = \frac{C_L - C_S}{C_S} = \frac{I_S}{I_L} - 1, \quad (14)$$

$$e_H = \frac{C_H - C_S}{C_S} = \frac{I_S}{I_H} - 1. \quad (15)$$

The errors e_Y , e_{YL} , e_L and e_H are plotted in Fig. 4 for w/t_0 ranging from 0.0001 to 1. From Fig. 4 we learned that

- The errors between the C_S and C_Y are less than 0.5%.
- C_L may result in errors up to 14% as w/t_0 approaches 1.
- The maximum error between I_{YL} and I_L is about 0.8% as w/t_0 approaches 1, which agrees with the statement in [10].
- C_H is easy to use but may result in a large error (up to 17%).

4. Improved equations with symmetric relation of t_0 and w

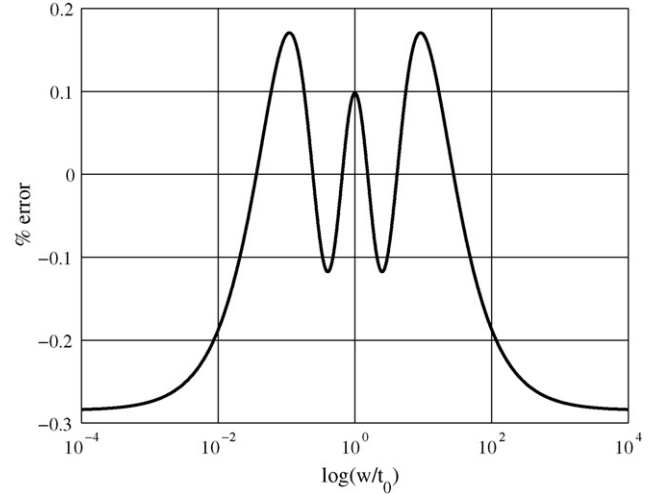
It is hypothesized that it is possible to create a relationship that, like Eq. (11), is symmetric with t and w , but has increased accuracy. This section develops this as an equation for a leaf-type flexure and also is used to develop a more general relationship for variable cross-sections. Let $z = w/t$. Leaf-type flexure hinges have constant w and t_0 , and $z_0 = w/t_0$. To improve the calculation precision of C_H while not overly complicating the analytical equation, a compensatory function is introduced. This compensation function is a function of z and is denoted by $f(z)$:

$$I_C = f(z)I_H. \quad (16)$$

In addition, in order to maintain the symmetric feature of I_H , $f(z)$ ought to bear the same symmetric relation between t_0 and w , that is to say, $f(z) = f(1/z)$.

According to Eq. (15), we want

$$e_C = \frac{I_S}{f(z)I_H} - 1 = 0. \quad (17)$$

Fig. 5. Errors of C_C compared to C_S as a function of the width-to-thickness ratio w/t_0 .

Combining Eqs. (15) and (17) yields

$$f(z) = e_H + 1. \quad (18)$$

Two steps were followed to determine $f(z)$:

- First, e_H was extended from [0.0001,1] to [0.0001,10000]. The data in the region from [1,10000] was mapped using $f(z) = f(1/z)$.
- Second, a rational quadratic polynomial fitting was performed to find the numerator and the denominator for $f(z)$, which yields

$$f(z) = \frac{1.17z^2 + 2.191z + 1.17}{z^2 + 2.609z + 1}. \quad (19)$$

Therefore, the improved compliance equation for leaf-type flexure hinges ($z = z_0$) can be expressed as

$$C_C = \frac{C_H}{f(z_0)} = \frac{7l}{2Gf(z_0)} \left(\frac{1}{t_0 w^3} + \frac{1}{t_0^3 w} \right), \quad (20)$$

and the errors of C_C compared to C_S are plotted in Fig. 5. The largest error is less than 0.28% when z spans from 0.0001 to 10000. That is to say, C_C is more accurate than C_Y (and thus also more accurate than C_{YL} , C_L and C_H) while calculating torsional deformation. In addition to having an improved accuracy over other equations, the relative magnitude of w and t are not important in the equation.

Even better fitting results may be achieved with a 5th degree polynomial numerator and 5th degree polynomial denominator (denoted it as $f'(z)$):

$$f'(z) = \frac{1.167z^5 + 29.49z^4 + 30.9z^3 + 100.9z^2 + 30.38z + 29.41}{z^5 + 25.91z^4 + 41.58z^3 + 90.43z^2 + 41.74z + 25.21}, \quad (21)$$

and the corresponding compliance equation for leaf-type flexure hinges can be expressed as

$$C'_C = \frac{C_H}{f'(z)} = \frac{7l}{2Gf'(z)} \left(\frac{1}{t_0 w^3} + \frac{1}{t_0^3 w} \right). \quad (22)$$

The errors of C'_C compared to C_S are less than 0.03%, as shown in Fig. 6. But Eq. (21) is too complex for practical use. The quadratic polynomial of Eq. (19) is sufficient for most applications.

These two general torsional compliance equations for leaf-type flexure hinges C_C and C'_C , maintain the symmetric relation between w and t_0 and are more accurate than C_H . C_C and C'_C also apply to

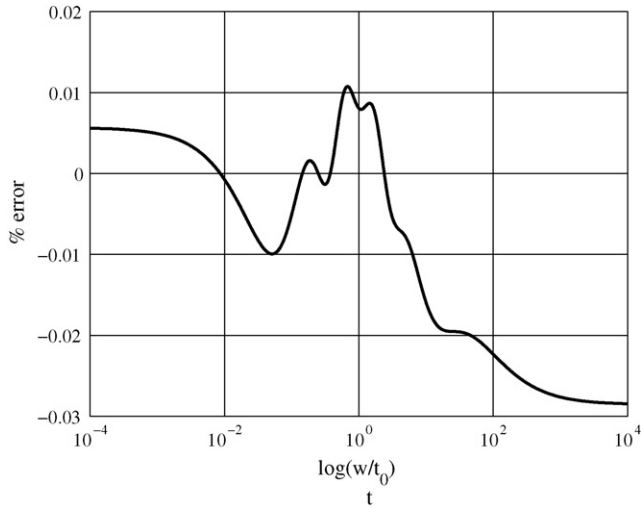


Fig. 6. Errors of C'_C compared to C_S as a function of the width-to-thickness ratio w/t_0 .

variable rectangular cross-section beams because every infinitesimal strip along the length of the beam can be treated as a constant cross-section beam.

The equations for leaf-type flexure hinges provide a foundation for the derivation of the torsional compliance for variable rectangular cross-sections. Allowing for both flexure thickness and width to vary as a function of x and substituting Eq. (11) into Eq. (2) yields

$$C_H = \int_0^l \frac{7}{2G} \left[\frac{1}{w^3(x)t(x)} + \frac{1}{w(x)t^3(x)} \right] dx \quad (23)$$

The accuracy of this equation can be improved by using I_C in Eq. (2), results in

$$C_C = \int_0^l \frac{7}{2G} \left[\frac{1}{w^3(x)t(x)f(t(x)/w(x))} + \frac{1}{w(x)t^3(x)f(t(x)/w(x))} \right] dx \quad (24)$$

or if the more complex $f'(x)$ is used, the torsional compliance is

$$C'_C = \int_0^l \frac{7}{2G} \left[\frac{1}{w^3(x)t(x)f'(t(x)/w(x))} + \frac{1}{w(x)t^3(x)f'(t(x)/w(x))} \right] dx \quad (25)$$

Eqs. (24) and (25) provide general equations for the torsional compliance of variable rectangular cross-sections and are still symmetric in w and t because $f(z) = f(1/z)$ and $f'(z) = f'(1/z)$.

5. Torsional compliance equation for single-axis elliptical and circular flexure hinges of variable rectangular cross-sections

The two general torsional equations can be demonstrated by deriving the torsional compliance for elliptical flexure hinges. A discussion of flexure geometry is followed by the derivation of a symmetric relation for torsional compliance based on I_H . This is followed by the derivation of another symmetric relationship, based on I_C , that has improved accuracy compared to that developed using I_H .

As shown in Fig. 7, the thickness of the infinitesimal strip (dx) at position x for an elliptical flexure hinge can be expressed as

$$t(x) = 2b + t_0 - \frac{2b}{a} \sqrt{2ax - x^2}, \quad (26)$$

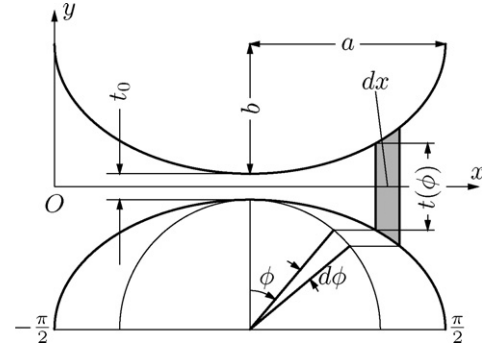


Fig. 7. Analysis of the profile of elliptical flexure hinge.

and the width is a constant, with $w(x) = w$. In order to simplify the deduction of the torsional compliance equation for elliptical hinges, eccentric angle ϕ was introduced as the integral variable. For

$$x = a + a \sin \phi, \quad (27)$$

Eq. (26) can be rearranged to yield

$$t(\phi) = 2b + t_0 - 2b \cos \phi. \quad (28)$$

Differentiation of Eq. (27) yields

$$dx = d(a \sin \phi) = a \cos \phi d\phi. \quad (29)$$

By substituting Eqs. (27)–(29) into Eq. (23), the symmetric torsional compliance equation [13] can be expressed as

$$C_H = \int_{-\pi/2}^{\pi/2} \frac{7}{2G} \left[\frac{a \cos \phi}{w^3 t(\phi)} + \frac{a \cos \phi}{w t^3(\phi)} \right] d\phi. \quad (30)$$

Supposing $s = b/t_0$ and substituting it into Eq. (28), the strip height at position ϕ can be expressed as

$$p(\phi) = t(\phi)/b = 2 + 1/s - 2 \cos \phi. \quad (31)$$

Substituting Eq. (31) into Eq. (30) yields

$$\begin{aligned} C_H &= \frac{7a}{2Gw^3b} \int_{-\pi/2}^{\pi/2} \frac{\cos \phi}{p(\phi)} d\phi + \frac{7a}{2Gwb^3} \int_{-\pi/2}^{\pi/2} \frac{\cos \phi}{p^3(\phi)} d\phi \\ &= \frac{7a}{2Gwb} \left(\frac{N_1}{w^2} + \frac{N_2}{b^2} \right), \end{aligned} \quad (32)$$

where

$$N_1 = \frac{2(2s+1)}{\sqrt{4s+1}} \arctan \left(\sqrt{4s+1} \right) - \frac{\pi}{2}, \quad (33)$$

$$N_2 = \frac{2s^3(6s^2+4s+1)}{(4s+1)^2(2s+1)} + \frac{12s^4(2s+1)}{(4s+1)^{5/2}} \arctan \sqrt{4s+1}. \quad (34)$$

By substituting $w(x) = w$ into Eq. (24), the torsional compliance is given by

$$C_C = \int_0^l \frac{7}{2Gw^3t(x)f[t(x)/w]} dx + \int_0^l \frac{7}{2Gwt^3(x)f[t(x)/w]} dx. \quad (35)$$

Like C_Y , the C_C and C'_C equations are still difficult if not impossible to integrate in their original form for variable cross-section hinges because of the high-degree items in the integration. If high-calculation precision is required, numerical integration methods should be used to determine the compliance (denoted by C_C). However, unlike C_Y , it requires no switch of $t(x)$ and w .

The integration of the equation is made easier by simplifying the compensation function, $f(z)$. Using $z_0 = t_0/w$ instead of $z = t(x)/w$ in the compensation function, $f(z)$, while maintaining a variable thickness, $t(x)$, elsewhere, simplifies the integration with little loss

Table 2
Torsional compliance calculations for several examples using various methods

Example	Type	w (mm)	b (mm)	C _S	C _Y	C _L	C _H	C _C	C _{CS}
1	Leaf	0.08	0	965.05	965.02	965.02	1065.48	966.67	966.67
2	Leaf	0.8	0	2.1441	2.1402	2.4439	2.1099	2.1462	2.1462
3	Leaf	8	0	0.0965	0.0965	0.0965	0.1065	0.0967	0.0967
4	Circular	0.5	5	2.3240	2.3230	2.3300	2.3673	2.3232	2.3869
5	Circular	0.01	5	212995	212995	212995	247238	212559	213215
6	Circular	0.08	5	431.74	431.73	431.73	485.28	432.10	440.28
7	Circular	0.7	5	0.9965	0.9984	1.0210	0.9990	0.9967	1.0155
8	Circular	0.8	5	0.7279	0.7288	0.7680	0.7263	0.7282	0.7388
9	Circular	2	5	–	–	–	0.1283	0.1278	0.1266
10	Circular	6	5	–	–	–	0.03361	0.03136	0.03095
11	Circular	10	5	–	–	–	0.01972	0.01790	0.01772
12	Circular	11	5	0.01615	0.01615	0.01615	0.01789	0.01617	0.01601
13	Circular	10.8	5	0.01647	0.01647	0.01647	0.01823	0.01649	0.01632
14	Circular	15	5	0.01164	0.01164	0.01164	0.01306	0.01165	0.01156
15	Circular	20	5	0.00863	0.00863	0.00863	0.00977	0.00864	0.00858
16	Circular	50	5	0.00338	0.00338	0.00338	0.00390	0.00338	0.00337
17	Elliptical	0.5	3	2.7985	2.7973	2.8063	2.8372	2.7974	2.8607
18	Elliptical	0.01	3	252230	252229	252229	292695	251724	252416
19	Elliptical	0.08	3	512.35	512.34	512.34	574.72	512.86	521.42
20	Elliptical	0.7	3	1.2092	1.2116	1.2407	1.2074	1.2094	1.2273
21	Elliptical	0.8	3	0.8865	0.8877	0.9381	0.8815	0.8869	0.8967
22	Elliptical	2	3	–	–	–	0.1605	0.1600	0.1584
23	Elliptical	4	3	–	–	–	0.06655	0.06366	0.06280
24	Elliptical	6	3	–	–	–	0.04267	0.03979	0.03930
25	Elliptical	11	3	0.02052	0.02052	0.02052	0.02276	0.02055	0.02036
26	Elliptical	10.8	3	0.02093	0.02093	0.02093	0.02319	0.02096	0.02076
27	Elliptical	15	3	0.01480	0.01480	0.01480	0.01661	0.01482	0.01471
28	Elliptical	20	3	0.01098	0.01098	0.01098	0.01243	0.01098	0.01092
29	Elliptical	50	3	0.00431	0.00431	0.00431	0.00496	0.00430	0.00429

For all the designs $t_0 = 0.8$ mm, $a = 5$ mm and $G = 8.1 \times 10^{10}$ N/m².

of accuracy. The simplification is a reasonable assumption because the deformation of a hinge is mainly distributed at the most flexible part of the notch region. Because z_0 is a constant for a specific hinge, $f(z_0)$ can be moved outside the integration in Eq. (2). The compliance equation can be expressed as

$$C_{CS} = \frac{z_0^2 + 2.609z_0 + 1}{1.17z_0^2 + 2.191z_0 + 1.17} \left(\frac{7a}{2Gwb} \right) \left(\frac{N_1}{w^2} + \frac{N_2}{b^2} \right), \quad (36)$$

The torsional compliance equation for elliptical hinges, C_{CS} , is a symmetric relationship that does not depend on the relative magnitude of w and t , is more accurate than C_H , and does not require numerical integration for calculation. A similar equation can be developed by using $f'(z_0)$ rather than $f(z_0)$.

The equations for C_C and C_{CS} also apply to circular hinges by applying $a = b$.

6. Torsional compliance calculations using various equations

The torsional compliance was calculated for all the methods described here for 29 different example designs. The parameters describing these designs are listed in Table 2. Designs 1–3 are leaf-type hinges, 4–16 are circular hinges and 17–29 are elliptical hinges. The torsional compliance C_S , C_Y and C_C were calculated by using high-precision numerical integration, while the C_L [10], C_H , and C_{CS} were calculated by using the closed-form equations. The results are listed in Table 2. There are several grids in Table 2 left blank, which is because there are switch points in the designs (piecewise integration is needed) not accounted for by certain equations.

From the results we may conclude that:

- C_S , C_Y and C_L are dependent on the relative magnitude of w and $t(x)$;

- C_H , C_C and C_{CS} do not depend on the the relative magnitude of w and $t(x)$;
- The errors of the results of C_L are the largest when w/t_0 approaches 1;
- The errors of the results of C_H become the largest when $w/t_0 \ll 1$ or $w/t_0 \gg 1$;
- C_C is more accurate than C_H but difficult to integrate;
- The simplified version of C_C , i.e., C_{CS} , is more accurate than C_H and only slightly less accurate than C_C and integrable.

7. Application example

Consider an example to illustrate the application of the compliance equation in an application. Fig. 8 shows a parallel-guiding mechanism utilizing elliptical flexure hinges. The device is fabricated from a single planar layer but provides micromotion out of that plane. All the elliptical flexure hinges are of the same size

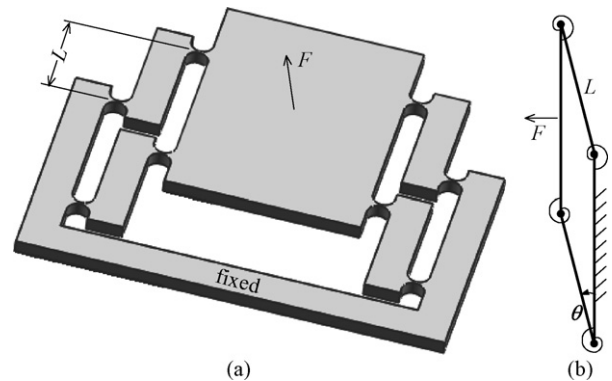


Fig. 8. A parallel-guiding mechanism: (a) its 3D model and (b) its pseudo-rigid-body model illustrates the resulting motion.

and are mainly subject to torsion when a force, F , is applied. The parameters of the mechanism are given as following:

- $L = 0.05$ m
- $w = 0.006$ m
- $a = 0.005$ m
- $b = 0.003$ m
- $t = 0.0008$ m
- $G = 8.1 \times 10^{10}$ N/m²

The center platform will remain horizontal during the motion (as illustrated in Fig. 8b) and the angular rotation of the side segments is measured by the angle θ . The compliance equation C_{CS} (Eq. (36)), and the device geometry, are utilized to find out the relationship between force F and angle θ . The resulting equation can be expressed as

$$F = \frac{8\theta}{C_{CS}L \cos \theta} = 4071.2 \frac{\theta}{L \cos \theta} \quad (37)$$

If C_H is used instead of C_{CS} in Eq. (37), F will be

$$F = \frac{8\theta}{C_H L \cos \theta} = 3749.7 \frac{\theta}{L \cos \theta} \quad (38)$$

8. Conclusions

Several existing equations for torsional compliance of rectangular cross-sections have been reviewed and compared. Two new equations for calculating the torsional compliance have been proposed. These equations are independent of the relative magnitude of the cross-section thickness and width, making them particularly well suitable for calculation of the torsional compliance of variable rectangular cross-section beams and design optimization of torsional hinges. The closed-form equation for the torsional compliance of elliptical and circular flexure hinges was derived.

Acknowledgements

The authors would like to thank the reviewers and the editor for their valuable comments. This research is supported by the National Natural Science Foundation of China under Grant No. 50805110

and the China Postdoctoral Science Foundation under Grant No. 20070421110.

References

- [1] Jacobsen JO, Howell LL, Magleby SP. Components for the design of lamina emergent mechanisms. Proceedings of IMECE 2007: IMECE2007-42311.
- [2] Goldfarb M, Speich JE. A well-behaved revolute flexure joint for compliant mechanism design. Journal of Mechanical Design, Transaction of ASME 1999;121:424–9.
- [3] Degani O, Socher E, Lipson A, Leitner T, Setter DJ, Kaldor S, et al. Pull-in study of an electrostatic torsion microactuator. Journal of Microelectromechanical Systems 1998;7:373–9.
- [4] Bao MH, Sun YC, Zhou J, Huang YP. Squeeze-film air damping of a torsion mirror at a finite tilting angle. Journal of Micromechanics and Microengineering 2006;16:2330–5.
- [5] Howell LL. Compliant mechanisms. New York: Wiley; 2001.
- [6] Koseki Y, Tanikawa T. Kinematic analysis of translational 3-DOF microparallel mechanism using matrix method. In: Proceedings of IEEE RSJ Conference. 2000. p. 1584–9.
- [7] Young WC, Budynas RG. Roark's Formulas for Stress and Strain. 7th ed. New York: McGraw Hill; 2002.
- [8] Lobontiu N, Garcia E. Two microcantilever designs: lumped-parameter model for static and modal analysis. Journal of Microelectromechanical Systems 2004;13:41–50.
- [9] Lobontiu N, Ilic B, Garcia E, Reissman T, Craighead HG. Modeling of nanofabricated paddle bridges for resonant mass sensing. Review of Scientific Instruments 2006;77:073301–9.
- [10] Lobontiu N, Garcia E, Canfield S. Torsional stiffness of several variable rectangular cross-section flexure hinges for macro-scale and MEMS applications. Smart Materials and Structures 2004;13:12–9.
- [11] Paros JM, Weisbord L. How to design flexure hinges. Machine Design 1965;37:151–6.
- [12] Smith ST, Badami VG, Dale JS, Xu Y. Elliptical flexure hinges. Review of Scientific Instruments 1997;68:1474–83.
- [13] Hearn EJ. Mechanics of materials. Oxford: Pergamon Press; 1977.
- [14] Hall AS. An introduction to the mechanics of solids. New York: John Wiley & Sons; 1969.
- [15] Shames IH, Pitarresi JM. Introduction to solid mechanics. 3rd ed. New Jersey: Prentice Hall; 2000.
- [16] Timoshenko SP, Gere JM. Strength of materials. New York: Van Nostrand; 1958.
- [17] Marin J, Sauer JA. Strength of materials. 2nd ed. New York: Macmillan Company; 1954.
- [18] Cook RD, Young WC. Advanced mechanics of materials. New York: Macmillan Company; 1985.
- [19] Bauld NR. Mechanics of materials. California: Brooks; 1982.
- [20] Timoshenko SP, Goodier JN. Theory of elasticity. 3rd ed. New York: McGraw-Hill; 1970.
- [21] Asaro RJ, Lubarda VA. Mechanics of solids and materials. Cambridge: Cambridge University Press; 2006.